LAMBDA PHYSIK®

LAMBDA HIGHLIGHTS

A PUBLICATION BY LAMBDA PHYSIK · JULY 2002 · No. 60

Laser-Induced Surface Patterning by means of Microspheres

Dieter Bäuerle, Klaus Piglmayer, Richard Denk, Nikita Arnold
Angewandte Physik, Johannes-Kepler-Universität Linz, Austria

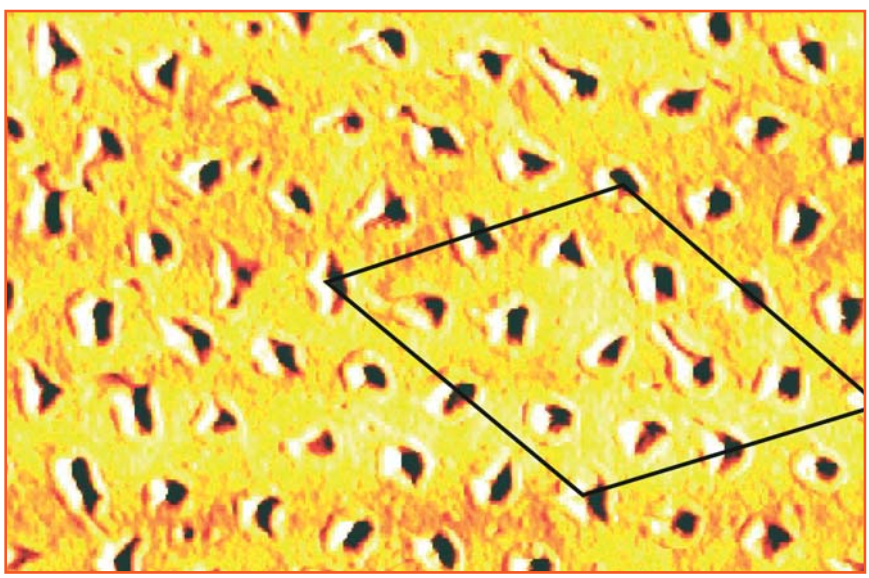

Fig. 4: AFM picture of holes produced by single-shot KrF-laser ablation of PI. The substrate was placed at a distance $z = f + \varepsilon$ with $\varepsilon \approx 2.7\,\mu m$. The arrangement of holes is equal to that of the interference maxima in Fig. 2b (see rhombus).

Within the last two decades micron- and submicron patterning of material surfaces by laser-induced ablation, etching, deposition, and surface modification has been extensively investigated [1]. Here, patterning was performed by "direct writing" where the laser light is just focused onto the substrate, by projection of the laser light via a mask, by employing a direct-contact mask, or by the interference of laser beams. Another technique employs a **SNOM**-type (***s***canning ***n***ear field ***o***ptical ***m***icroscope) setup. Here, the laser light is coupled into the tip of a solid or hollow fiber. By positioning the substrate within the near field of the fiber tip, one can produce patterns with widths that are not limited by optical diffraction. This technique has been employed for nanolithography [2], ablation [3], material etching [4] and for local reduction of oxides [5]. Its main disadvantage is the low throughput that can be achieved in a fabrication process, even when bundles of fibers are used.

Presently, we are investigating a new method for single step maskless patterning. It permits one to produce on a substrate surface thousands or millions of single submicron features with a single or a few laser shots. The technique employs a regular two-dimensional (2D) lattice of microspheres. Such lattices are formed by well-known self-assembly processes, e.g. from colloidal suspensions. In contrast to earlier investigations [6] we used such 2D lattices not as lithographic masks for consecutive processes, but as an array of microlenses on a transparent support. The microspheres focus the incident laser radiation onto the substrate, albeit with significant (spherical) aberration. The

IN THIS ISSUE:

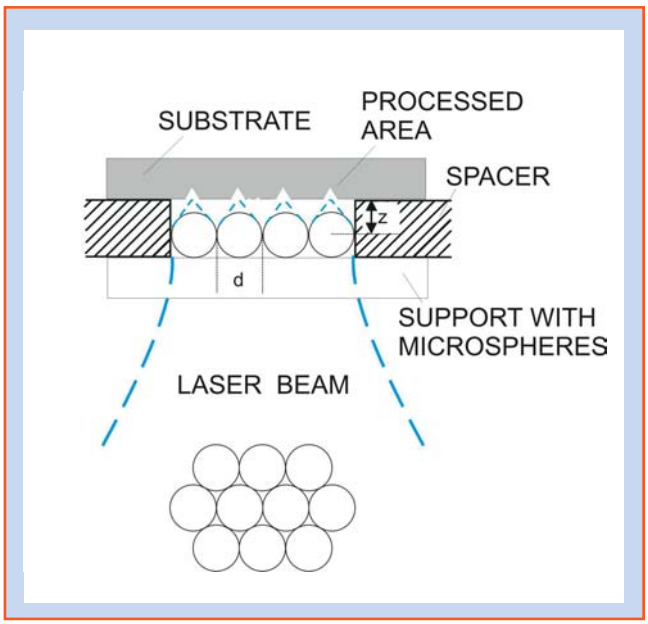

Fig. 1: Schematic picture of the setup employed in the experiments. The transparent microspheres of diameter d = 2r focus the incident laser radiation onto the substate surface [7].

experimental arrangement employed is schematically shown in ***Fig. 1***. According to geometrical optics, the "focal plane" of microspheres, i.e. the distance between their centers where both principal planes are positioned, and their foci, f, is given by

$$f \approx \frac{r}{2}\,\frac{n}{n-1} \qquad (1)$$

where r is the radius and n the refractive index of the microspheres. A white light image generated by a-SiO_2 microspheres at a distance $z = f$ is shown in ***Fig. 2a***. In this case, the microscope picture reveals the hexagonally close-packed structure of the lattice formed by the microspheres. The distance between intensity maxima is equal to the diameter of microspheres which was $d = 2r = 3 \pm 0.15\,\mu m$. With n(a-SiO_2) = 1.50, we find for the distance of the focal plane $z \approx 2.25\,\mu m$. In reality, spherical aberration shifts the (diffraction) focus towards the spheres to a position $f_d \approx f(1-C\sqrt{\lambda/r})$ where λ is the wavelength and $C(n)$ a constant. Simultaneously, aberration decreases the maximum intensity (fluence) within the focus from $I_f/I_0 \propto (r/\lambda)^2$ to $I_d/I_0 \propto r/\lambda$ [9,10]. From numerical calculations one obtains for the parameters employed in our experiments $z \approx f_d \approx 1.75\,\mu m$, and $I_d/I_0 \approx 150$.

The experimental setup shown in ***Fig. 1*** can be used for photoenhanced patterning of material surfaces. Here, we employ monolayers of a-SiO_2 microspheres on fused quartz supports. Clearly, the maximum laser fluence that can be used in such experiments has to be well below the threshold fluence for the detachment of the spheres from the support. The threshold fluence in laser cleaning experiments, where one has a similar situation, was found to increase with decreasing particle size [1,11].

The process studied in most detail is the ablation of polymers by means of excimer-laser radiation. ***Fig. 3*** shows an atomic force microscope (AFM) picture of a small part of a polyimide (PI) foil patterned with single-shot 248 nm KrF-laser radiation. The fluence was $\phi \approx 50\,mJ/cm^2$ and the pulse length at full width half maximum (FWHM) $\tau_\lambda \approx 28\,ns$. With these laser parameters, we observe strong ablation of the polymer foil within the foci of the microspheres. The holes shown in the figure have a FWHM diameter of 500 ± 100 nm and a depth of 250 ± 50 nm. Their mean distance is equal to the mean diameter of the microspheres. The arrangement of holes clearly reveals the hexagonal lattice structure of the microspheres. By using microspheres of various diameters, the distance between holes can be varied by at least two orders of magnitude. Similar experiments have been performed with other materials. However, in contrast to most other polymers as, e.g., polyethyleneterephthalate (PET), PI does not melt, but directly sublimates into gaseous product species.

The microscopic mechanisms of photoablation of polymers have been discussed in detail in [1]. For PI and 302 nm laser radiation with pulse lengths between 10 ns ≤ τ_λ ≤ 1s we found that ablation can be quantitatively described by purely thermal mechanisms [12].

Interference Subpatterns

If we now vary the distance z by an amount ε, so that the total distance between the center of the microspheres and the substrate surface is given by $z = f + \varepsilon$, we can generate different interference patterns in the Fresnel region, which show periodically ordered well-defined maxima of similar intensities. The distances between these maxima are much smaller than the diameter of the spheres. This can be seen in the white-light microscope picture shown in ***Fig. 2b***. ***Fig. 4*** shows an AFM picture of a small part of a PI foil that has been patterned at $\varepsilon \approx 2.7 \pm 0.5\,\mu m$. It can be seen that the ablation pattern, i.e. the spatial arrangement of holes nicely reproduces the interference pattern in Fig. 2b (see the holes and interference maxima within the rhombus). From AFM profiles we find that the holes have a spacing of 805 ± 70 nm, a width at FWHM of 160 ± 40 nm and a depth of 100 ± 20 nm. The large inaccuracies in these values and the irregular shape of holes can be related to the roughness and thickness variations of the PI foil, the size distribution of spheres and polarization effects. These effects cause locally different focusing, aberration and interference.

The changes in the spatial frequency of the hexagonal pattern can be qualitatively understood along the following lines. Spheres create waves, which first converge, and then diverge behind the foci. These waves interfere in the region where

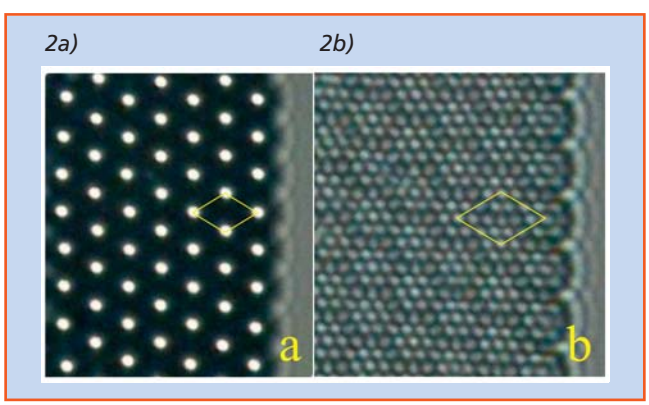

Fig. 2: White-light microscope pictures generated by a-SiO_2 microspheres of diameter $d = 3 \pm 0.15\,\mu m$. a) $z \approx f$; in this case the distance between the intensity maxima is equal to the diameter of spheres. b) $z = f + \varepsilon$. The distance between interference maxima is about 800 nm. At the right side of the figures the boundary of the array of spheres can be seen [8].

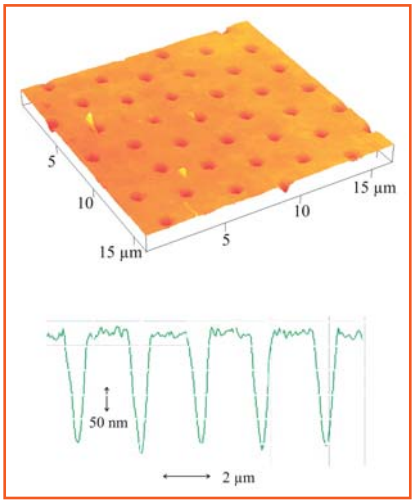

Fig. 3: Holes produced by local KrF-laser-induced ablation of PI (polyimide) in the focal plane of a-SiO_2 microspheres (d = 3 ± 0.15µm). The lower part shows the (uncorrected) depth profile of holes measured by means of an AFM.

they significantly overlap. Due to their localization, only adjacent beams will interact. Let us approximate each beam by a Gaussian field distribution. The superposition of these single beams yields an interference pattern. The resulting intensity distribution depends on the two-dimensional vector ρ within planes z = const and it is given by

$$I(\tilde{n}) \propto \left| \sum_j A(|\rho - \rho_j|) \exp\left[\frac{ik|\rho-\rho_j|^2}{2R(z)} \right] \right|^2 \quad (2)$$

Here, all factors that are identical for all beams have been omitted. $R \equiv R(z)$ is the radius of curvature of beams and A the amplitude. ρ_j describes the center of beam number j. The calculated intensity distribution is shown in ***Fig. 5***. Consider, e.g., the interference of 3 adjacent beams with spacing d. Interference will be constructive if the phases of beams $\frac{k|\rho-\rho_j|^2}{2R}$, differ by $2\pi m$, where m is an integer. For the points 1 and 2 in ***Fig.5b***, this results in

$$R = \frac{d^2}{4\pi m}$$

which was used in the calculations with m = 1. The primary maxima which are also observed within the focal plane, are indicated by a "0" and secondary (additional) maxima by "1" and "2". Both, primary and secondary maxima have similar intensities, as they are created by about the same number of interfering beams.

While the calculated intensity distributions shown in Figs. 5a,b qualitatively describe the pictures in Figs. 2a,b and the arrangement of generated patterns in Figs.3 and 4 quite well, a *direct*, quantitative comparison is not possible. This has several reasons: The differences in wavelengths employed, the omission of aberration phenomena in the theoretical considerations, the size distribution of microspheres, the uncertainties in the material and experimental parameters, etc. The interference patterns before and behind the focal point may differ significantly. Arrays of spheres can be considered as a diffraction grating. The field distribution *in the Fresnel region* is quite complicated and is governed by the parameter d^2/λ (Talbot effect [13]).

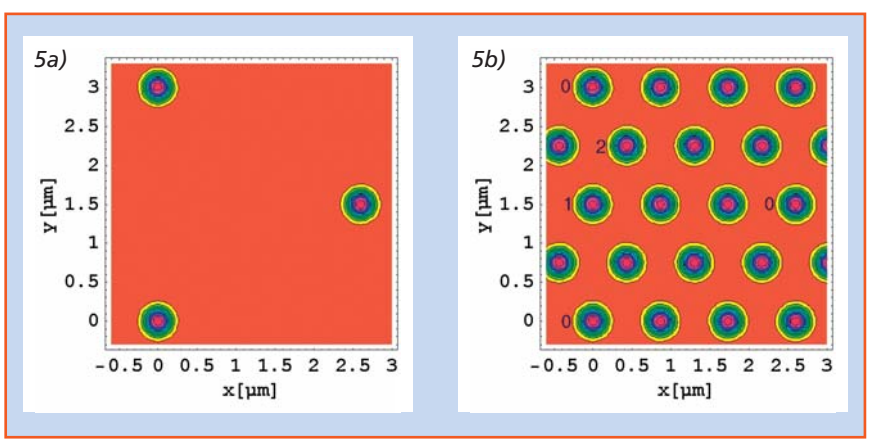

Fig. 5: Interference pattern generated by superposition of Gaussian beams. The wavelength employed is λ= 0.248µm and the Rayleigh length z_R=3λ. This corresponds to a beam waist w_o(1/e field at z = f) = $\sqrt{3/\pi}\lambda$ = 0.242 µm. a) Intensity distribution within the focal plane z = f. b) Same as a) but at z = f + ε . At that position, the radius of curvature of waves is given by R(z) ≡ ε + z_R^2/ ε = $d^2/4\lambda$; ε = 9.01 µm. Though about 50 adjacent beams were used in the numerical summation, only the nearest neighbors significantly contribute to the interference pattern as the beam waist w (1/e field at z = f + ε) =2.94 µm.

In summary the technique described in this contribution can be employed for large-area surface patterning of substrates. In preliminary experiments we have demonstrated that the same technique can be used for laser-induced chemical etching, deposition, and surface modification. In contrast to "direct writing", thousands or millions of single submicron features can be produced with a single or a few laser shots.

Acknowledgements

We wish to thank the Austrian 'Bundesministerium für Verkehr, Innovation und Technologie', project #GZ 602.513/4-V/A/5/2001 for financial support.

Dieter Bäuerle
Angewandte Physik,
Johannes-Kepler-Universität Linz
A-4040 Linz, Österreich
Tel. ++43 2468 9244,-9243
Fax. ++43 2468 9242
E-mail: dieter.baeuerle@jku.at

References

[1] D. Bäuerle: *Laser Processing and Chemistry*, 3rd edition, Springer Verlag 2000

[2] M.K. Herndon, R.T. Collins, R.E. Hollingsworth, P.R. Larson, M.B. Johnson: Appl. Phys. Lett. **74**, 141(1999)

[3] S. Nolte, B.N. Chichkov, H. Welling, Y. Shani, K. Lieberman, H. Terkel: Opt. Lett. **24**, 914 (1999)

[4] G. Wysocki, S.T. Dai, T. Brandstetter, J. Heitz, and D. Bäuerle, Appl. Phys. Lett. **79**, 159 (2001)

[5] J.D. Pedarnig, H. Göttlich, R. Rössler, W.M. Heckl, D. Bäuerle: Appl. Phys. A **67**, 403 (1998)

[6] F. Burmeister, W. Badowsky, T. Braun, S. Wieprich, J. Boneberg, P. Leiderer: Appl. Surf. Sci. **144-145**, 461 (1999); J.C. Hulteen, R.P. Van Duyne: J.Vac. Sci. Technol. A **13**, 1553 (1995)

[7] R. Denk, K. Piglmayer, D. Bäuerle: Appl. Phys. A (2002a)

[8] R. Denk, K. Piglmayer, D. Bäuerle: Appl. Phys. A (2002b)

[9] Yu. A. Kravtsov, Yu. I. Orlov, *Geometrical optics of inhomogeneous media,* Springer Verlag, 1990

[10] M. Born, E. Wolf, *Principles of Optics*, 6th edition, Pergamon press, 1980

[11] T. Fourrier, G. Schrems, T. Mühlberger, J. Heitz, N. Arnold, D. Bäuerle, M. Mosbacher, J. Boneberg, and P. Leiderer, Appl. Phys. A **72**, 1 (2001)

[12] K. Piglmayer, E. Arenholz, C. Ortwein, D. Bäuerle: Appl. Phys. Lett. **73**, 847 (1998)

[13] M. Berry, I. Marzoli, W. Schleich, Physics World, June, 39, (2001)